Int J Adv Manuf Technol (2017) 88:683–690
DOI 10.1007/s00170-016-8803-1

ORIGINAL ARTICLE

Investigation of interface compatibility during ball spinning of composite tube of copper and aluminum

Shuyong Jiang[1] · **Yanqiu Zhang**[1] · **Yanan Zhao**[1] · **Xiaoming Zhu**[1] · **Dong Sun**[2] · **Man Wang**[2]

Received: 16 December 2015 / Accepted: 18 April 2016 / Published online: 27 April 2016
© Springer-Verlag London 2016

Abstract As a new attempt, ball spinning was used to manufacture a composite tube of copper and aluminum. The interface compatibility of the composite tube during ball spinning was investigated by combining finite element method with process experiment. The experimental results are in good agreement with the simulated ones. When the composite tubular blank which is composed of inner aluminum tube and outer copper tube is subjected to ball spinning, the composite tube keeps a good synchronism in terms of plastic deformation. When the composite tubular blank which consists of inner aluminum tube and outer copper tube undergoes ball spinning, the composite tube keeps a poor synchronism in terms of plastic deformation. The phenomenon indicates that the yield strength of the inner and outer tubes plays a significant role in the interface compatibility during ball spinning of the composite tube. According to the experimental and simulated results, the interface compatibility of the composite tube during ball spinning should meet the following requirements, including boundary condition of admissible velocity field, geometrical condition of composite tubular blank, steady flow condition of surface metal, and plastic yield condition of composite tube.

Keywords Finite element method · Metal forming · Ball spinning · Composite tube · Interface compatibility

✉ Shuyong Jiang
jiangshy@sina.com

[1] College of Mechanical and Electrical Engineering, Harbin Engineering University, Harbin 150001, China

[2] College of Materials Science and Chemical Engineering, Harbin Engineering University, Harbin 150001, China

1 Introduction

A composite tube, which is also called bimetallic tube or clad tube, is generally composed of two kinds of different metal materials. A composite tube is superior to a single tube made from the same metal material in terms of property and cost. In general, a composite tube can be manufactured by means of two methods, including metallurgical bonding and mechanical bonding. It is accepted generally that metallurgical bonding is based on atomic bonding between two metal materials. However, mechanical bonding is a term always used for mechanical locking of the contact surfaces of two metal materials as a result of surface roughness. The metallurgical bonding method contributes to enhancing the interface strength of a composite tube since it is able to implement the atomic diffusion bond between the two tubes. For example, the compound casting process becomes a representative candidate for fabricating the composite tube on the basis of metallurgical bonding methods as proposed by Jiang et al. [1]. However, the complicated process and the high cost impede the application of metallurgical bonding method in the engineering field. Mechanical bonding method is mainly based on plastic deformation and it has attracted more and more attention due to the simple process and the low cost. So far, many researchers have devoted themselves to manufacturing the composite tube by means of metal forming techniques. Knezevic et al. [2] fabricated the bimetallic tube of copper and aluminum by means of extrusion. Wang et al. [3] manufactured the bimetallic CRA-lined pipe, which has a liner pipe made of corrosion-resistant-alloy (CRA) and an outer pipe made of low-cost steel, by virtue of hydro-forming. However, the less plastic deformation degree leads to the weak interface bonding strength, so large plastic deformation plays an important role in enhancing the interface bonding strength of a composite tube. Consequently, the processes used for manufacturing a composite tube occur on the basis of high energy forming and large plastic deformation.

Guo et al. [4] successfully produced aluminum/steel clad tube with good bonding interface by means of explosive welding process. Yu et al. [5] manufactured Al-cladded mild steel tube with interfacial diffusion zone by virtue of magnetic pulse cladding process. Lapovok et al. [6] proposed a high-pressure tube twisting process leading to ultrafine-grained microstructure, which contributes to producing bimetallic tubes with a high-quality bonding interface.

As one of the near-net shape forming processes, metal spinning have been widely used for manufacturing axis-symmetrical, thin-walled, and hollow circular cross-section parts by exerting continuous and local plastic deformation on the sheet blank or tube blank as claimed by Xia et al. [7]. Power spinning, including shear spinning and tube spinning, manufactures the workpiece by changing the thickness of the blank. Ma et al. [8] manufactured the conical part with transverse inner rib by means of shear spinning. Haghshenas et al. [9] fabricated AISI 1020 steel workpiece with longitudinal internal ribs by means of a single-roller spinning forming over a splined mandrel. Ma et al. [10] selected appropriate ductile fracture criteria based on damage limit to accurately predict forming limit and damage evolution in tube spinning. Shan et al. [11] applied backward tube spinning to manufacture Ti-6Al-2Zr-1Mo-1V alloy tube and they investigated the evolution of the resultant texture and microstructure. In the recent study, metal spinning is also used to manufacture a composite tube. Mohebbi and Akbarzadeh [12] produced two-layered thin-walled Cu-Al composite tubes by means of tube spinning process, where severe shear strain plays an important role in enhancing the interface bonding strength of the composite tubes.

As a class of power spinning, ball spinning is the best candidate for manufacturing the thin-walled tube with high precision and high strength. Jiang et al. [13] applied ball spinning to manufacturing thin-walled aluminum alloy tube with longitudinal inner ribs. Furthermore, Jiang et al. [14] also manufactured NiTi shape memory alloy tube by virtue of ball spinning. Zhang et al. [15] manufactured the inner grooved copper tube with the aid of ball spinning. Kuss and Buchmayr [16] developed the ball spinning expansion process in order to manufacture lightweight austenite stainless tube.

In the present study, ball spinning is used to manufacture a composite tube of copper and aluminum, where the emphasis is laid on investigation of interface compatibility on the basis of ball spinning experiment and finite element method (FEM).

2 Experimental conditions

2.1 Spinning mode

The backward ball spinning was adopted in order to manufacture the composite tube of copper and aluminum, as shown in Fig. 1. The deformation zone is caused to be in a three-dimensional compressive stress state, which contributes to enhancing the workability of the metal material. The spinning tools are composed of spinning head and mandrel, where the spinning head consists of screw tube, outer die ring, bolt, and inner die ring. The spinning head was fixed in the chuck of the spinning lathe and turned with the principal axis of the spinning lathe during backward ball spinning. At the same time, the composite tubular blank was mounted on the mandrel and fed with the mandrel along the axial direction. Furthermore, the tapered inner surface is formed in the inner die ring. The gap between the balls and the mandrel can be changed by adjusting the axial position of the screw tube. As a consequence, the different wall thickness reduction can be implemented during ball spinning.

2.2 Spinning material

The composite tubular blanks used for spinning material are made up of commercial pure copper tube and pure aluminum tube, where the yield strength of copper tube is 430 MPa and the yield strength of aluminum tube is 146 MPa. Two kinds of composite tubular blanks were selected as spinning materials, as shown in Fig. 2. One kind of composite tubular blank is composed of the inner copper tube and the outer aluminum tube, where the inner copper tube possesses the length of 65 mm, the inner diameter of 24 mm and the wall thickness of 1 mm, while the outer aluminum tube possesses the length of 65 mm, the inner diameter of 26 mm and the wall thickness of 1 mm. The other kind of composite tubular blank is composed of the inner aluminum tube and the outer copper tube and its dimension is identical to that of the aforementioned composite tube except that the corresponding material is reversed. For the sake of convenience, in the following context, the composite tube made of an inner copper tube and an outer aluminum tube is expressed as a Cu-Al composite tube. Vice versa, the other composite tube is expressed as an Al-Cu

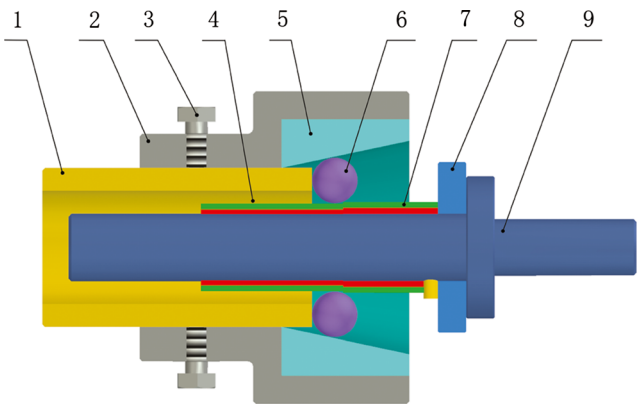

Fig. 1 Schematic diagram of backward ball spinning of a composite tube: *1* screw tube, *2* outer die ring, *3* bolt, *4* outer tube, *5* inner die ring, *6* ball, *7* inner tube, *8* stripper, *9* mandrel

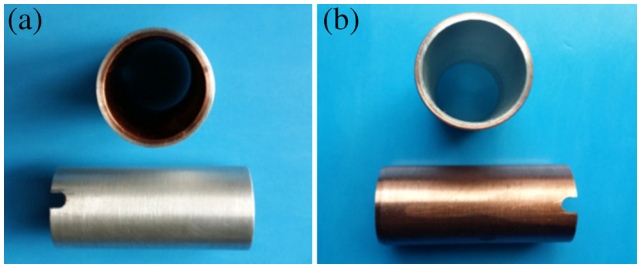

Fig. 2 Composite tubular blank used for backward ball spinning: **a** composite tube of an inner copper tube and an outer aluminum tube, **b** composite tube of an inner aluminum tube and an outer copper tube

composite tube. Furthermore, both the inner surface of the outer tube and the outer surface of the inner tube were brushed before the composite tubular blank was assembled. Simultaneously, the composite tubular blank was assembled by means of interference fit before ball spinning.

2.3 Spinning parameters

The involved process parameters during backward ball spinning were as follows. The feed ratio of the balls was 0.6 mm/r and the diameter of the balls was 18 mm. The wall thickness reduction was 0.6 mm. The number of the balls can be determined as seven according to the reference [17].

3 Finite element model

3.1 Fundamentals of rigid-plastic FEM

Rigid-plastic FEM is used for simulating ball spinning of a composite tube of copper and aluminum. Rigid-plastic FEM is based on the variational principles. The functional π is established as follows according to the plastic deformation body along with the incompressibility condition.

$$\pi = \int_V \overline{\sigma}\dot{\overline{\varepsilon}}\mathrm{d}V + \int_V \frac{\alpha}{2}\dot{\varepsilon}_v^2\mathrm{d}V - \int_S F_i u_i \mathrm{d}S \qquad (1)$$

Where V and S is the volume and the surface of the plastic deformation body, respectively, $\overline{\sigma}$ is the equivalent stress that is the function of the equivalent strain $\overline{\varepsilon}$, $\dot{\overline{\varepsilon}}$ is the equivalent strain rate, F_i is the surface tractions, u_i is the velocity field, $\dot{\varepsilon}_v$ is the volume strain rate, and α is the penalty factor that is a very large positive constant and in general ranges from 10^5 to 10^7.

Among admissible velocities that satisfy the conditions of compatibility as well as the velocity boundary conditions, the actual solution makes the first-order variation of the functional π vanish, namely:

$$\delta\pi = \int_V \overline{\sigma}\delta\dot{\overline{\varepsilon}}\mathrm{d}V + \alpha\int_V \dot{\varepsilon}_v\delta\dot{\varepsilon}_v\mathrm{d}V - \int_S F_i\delta u_i\mathrm{d}S = 0 \qquad (2)$$

Eq. (2) is the basic equation for the finite element discretization.

3.2 Finite element model

DEFORM-3D finite element code is used to simulate backward ball spinning of the composite tube. Finite element model of backward ball spinning of the composite tube is shown in Fig. 3, where seven balls are adopted according to the actual spinning experiment. The dimensions of the cross-section of the mandrel are identical to those in the experiment. The balls have a feed movement along the axial direction as well as a revolution movement along the circumferential direction, but the mandrel is constrained. The composite tubular blank possesses the free surface at the entrance end of the balls, while the tube blank possesses the constrained surface at the exit end of the balls. In addition, the interface between the inner tube and the outer tube can be considered as the relative movement surface. The frictional coefficients between the inner tube and the outer tube, between the inner tube and the mandrel, and between the outer tube and the balls are determined as 0.8, 0.12, and 0.08, respectively. The feed ratio of the balls is 0.6 mm/r, and the diameter of balls is 18 mm. The composite tubular blank with a length of 15 mm is used as finite element model, where the other dimensions are the same as those in the ball spinning experiment. The wall thickness reduction per pass is 0.6 mm. The outer tube consists of 55,580 elements and 16,264 nodes, while the inner tube is composed of 69,523 elements and 18,320 nodes.

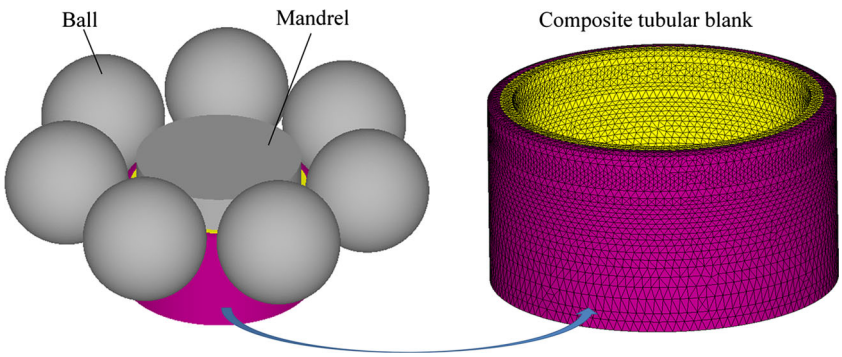

Fig. 3 Finite element model of backward ball spinning of composite tube

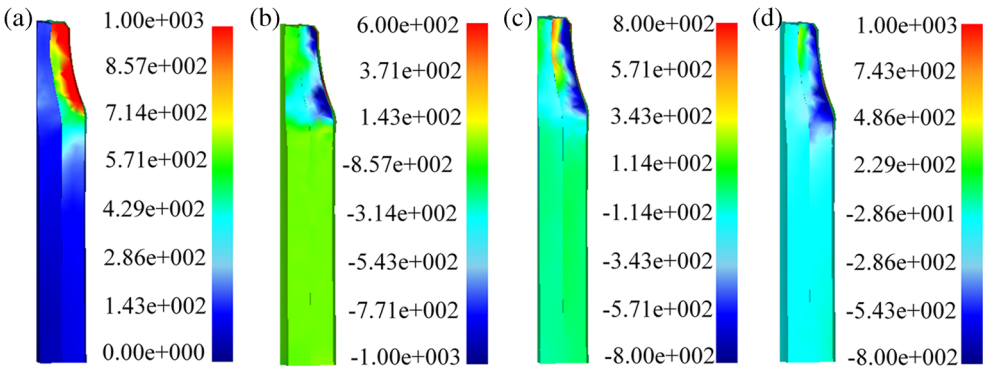

Fig. 4 Stress fields of Al-Cu composite tube derived from finite element simulation of ball spinning: **a** effective stress, **b** radial stress, **c** tangential stress, **d** axial stress

4 Results and discussion

4.1 Finite element simulation results

4.1.1 Ball spinning of an Al-Cu composite tube

Figures 4 and 5 show the stress field and the strain field of an Al-Cu composite tube derived from finite element simulation of ball spinning. It can be found from the effective stress distribution in Fig. 4 that the effective stress decreases gradually from the outer copper tube to the inner aluminum tube. Furthermore, it can be seen from the effective strain distribution in Fig. 5 that the effective strain decreases gradually from the outer copper tube to the inner aluminum tube, which reveals that the larger plastic deformation appears on the outer copper tube, while the less plastic deformation arises on the inner aluminum tube. It can be conclude that plastic strain distribution plays an important role in describing the level of plastic deformation during ball spinning of the composite tube. The phenomenon indicates that the outer copper tube of the composite tube satisfies plastic yield criterion more easily. In addition, the stress distribution in the entire thickness of outer copper tube and inner aluminum tube at a specific longitudinal section at a specific moment can be regarded as a function of the position of the balls at that moment. It can be observed from the radial stress field, the tangential stress field, and the axial stress field that the deformation zone before the balls is basically caused to be in a three-dimensional compressive stress state in the outer copper tube and the inner aluminum tube. However, the different stress distributions are imposed in the deformation zone of the outer copper tube and the inner aluminum tube right under the balls because there exists a friction between the outer copper tube and the inner aluminum tube. Furthermore, the interface between the outer copper tube and the inner aluminum tube is characterized by a material discontinuity. As a consequence, the tangential and longitudinal incompatibility between the outer copper tube and the inner aluminum tube would lead to a pair of opposite stresses in the two layers of tubes adjacent to the interface, where the tension stress is induced in the outer copper tube, while the compression stress is imposed in the inner aluminum tube. The phenomenon is attributed to the fact that there is a relative movement between the outer copper tube and the inner aluminum tube, which has an adverse influence on the interface compatibility between the outer copper tube and the inner aluminum tube.

It can be found from the radial strain field, the tangential strain field, and the axial strain field in the plastic deformation zone in Fig. 5 that the radial strain and the tangential strain are characterized by the compressive strain, while the axial strain belongs to the tensile strain. The compressive strain in the radial direction and the tensile strain in the axial direction contribute to the plastic flow of the metal material. However, the build-up of metal material on the surface of the composite tube occurs when the deformation zone is highly constrained in the tangential and axial directions [18]. In particular, when metal material builds up on the surface of the composite tube, the radial strain before ball

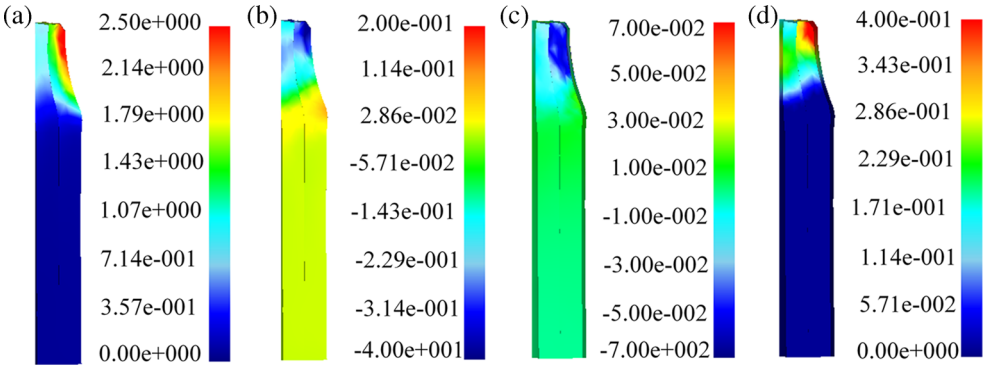

Fig. 5 Strain field of Al-Cu composite tube derived from finite element simulation of ball spinning: **a** effective strain, **b** radial strain, **c** tangential strain, **d** axial strain

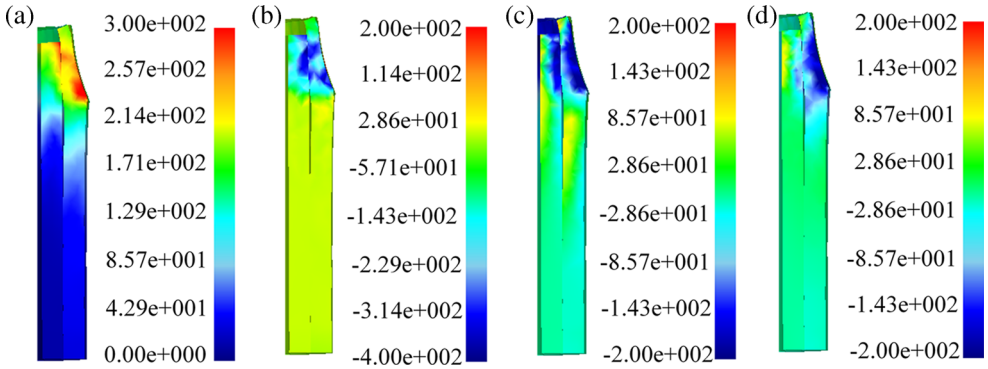

Fig. 6 Stress field of Cu-Al composite tube derived from finite element simulation of ball spinning: **a** effective stress, **b** radial stress, **c** tangential stress, **d** axial stress

belongs to the tensile strain, which has an adverse influence on the quality of the composite tube.

4.1.2 Ball spinning of a Cu-Al composite tube

Figures 6 and 7 show the stress fields and the strain fields of a Cu-Al composite tube derived from finite element simulation of ball spinning, respectively. Compared with an Al-Cu composite tube, the distribution of the stress and the strain in the deformation zone exhibits a certain similarity during ball spinning of a Cu-Al composite tube. However, in the case of interface compatibility, there exists an obvious difference between an Al-Cu composite tube and a Cu-Al composite tube. In particular, as for the Cu-Al composite tube, the inner copper tube is almost not subjected to plastic deformation, which is attributed to the fact that the spinning force is unable to be transmitted to the inner copper tube by means of the outer aluminum tube such that the inner copper tube does not meet the requirement for plastic yield criterion. As a consequence, only the outer aluminum tube is subjected to elongation deformation due to plastic yield, which has an adverse influence on the interface compatibility between the inner copper tube and the outer aluminum tube.

4.1.3 Prediction of spinning loading of Cu-Al and Al-Cu composite tubes

The spinning force during ball spinning of the composite tube can be divided into three spinning force components, including the radial spinning force component, the tangential spinning force component and the axial spinning force component. Figure 8 indicates the prediction curves of spinning loading of Cu-Al and Al-Cu composite tubes obtained by means of finite element simulation. It can be observed from Fig. 8 that the three spinning force components increase with the progression of the stroke of the ball in the form of the periodical variation. In particular, the spinning force components in the Al-Cu composite tube are much greater than the corresponding ones in the Cu-Al composite tube. The phenomenon further demonstrates that in the case of ball spinning of the Al-Cu composite tube, the inner aluminum tube, and the outer copper tube are subjected to plastic deformation such that a great deal of plastic work is consumed.

4.2 Experimental results of ball spinning

Figure 9 shows the Al-Cu composite tube and the Cu-Al composite tube obtained by means of ball spinning experiment. It can be found from Fig. 9 that the experimental results are in good agreement with the simulated ones. As for the Al-Cu composite tube, the inner aluminum tube, and the outer copper tube keep a good synchronism in terms of plastic deformation. However, in the case of the Cu-Al composite tube, the outer aluminum tube possesses the greater axial elongation compared with the inner copper tube. The phenomenon indicates that the yield strength of the inner and outer tubes plays a significant role in the interface compatibility during ball

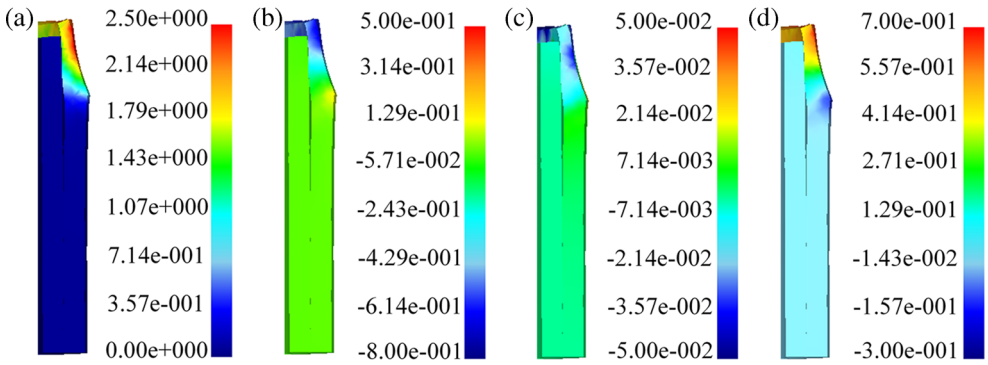

Fig. 7 Strain field of Cu-Al composite tube derived from finite element simulation of ball spinning: **a** effective strain, **b** radial strain, **c** tangential strain, **d** axial strain

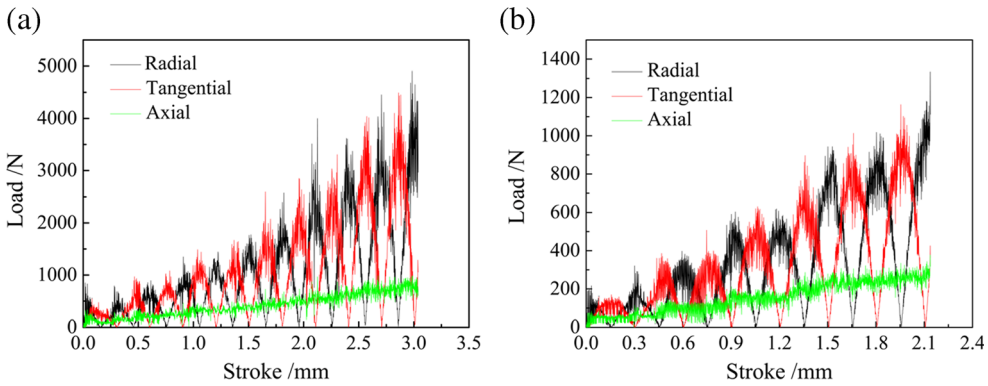

Fig. 8 Prediction of spinning loading of composite tubes: **a** Al-Cu composite tube, **b** Cu-Al composite tube

spinning of the composite tube. It can be noted from the aforementioned spinning materials that the yield strength of the copper tube is much higher than the one of the aluminum tube. Therefore, when the Al-Cu composite tube undergoes ball spinning, the plastic yield of the outer copper tube leads to the plastic yield of the inner aluminum tube. However, when the Cu-Al composite tube suffers from ball spinning, the outer aluminum tube is subjected to plastic yield prior to the inner copper tube such that the inner copper tube is almost unable to be subjected to plastic yield. Furthermore, when the Al-Cu composite tube is subjected to the larger ball spinning stroke, the inner aluminum tube is slightly longer than the outer copper tube, as shown in Fig. 10. The phenomenon indicates that the interface compatibility of the composite tube of copper and aluminum is also dependent on the other parameters, which are out of the scope of the paper.

4.3 Requirements for interface compatibility of a spun composite tube

In the present study, the Al-Cu composite tube and the Cu-Al composite tube are selected as the spinning materials, where the spinning material can be regarded as the only variable. As a matter of fact, the quality of the composite tube is influenced by many other factors, such as feed ratio, ball size, wall thickness reduction, geometry of tubular blank, friction condition, and so on. As a whole, the interface compatibility of the composite tube during ball spinning should meet the following requirements.

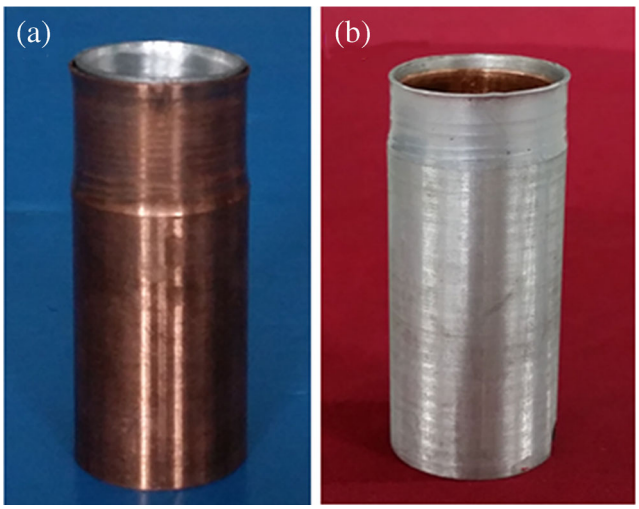

Fig. 9 Composite tubes obtained by means of ball spinning experiment: **a** Al-Cu composite tube, **b** Cu-Al composite tube

4.3.1 Boundary condition of admissible velocity field

Before ball spinning, the composite tubular blank is assembled on the basis of interference fit. In other words, the inner tube and the outer tube are bonded together by means of elastic and plastic deformation, where there is not relative movement between the inner tube and the outer tube. Therefore, the inner tube and the outer tube keep the same axial feed velocity as the mandrel. Furthermore, it can be assumed that the inner tube and the outer tube are bonded together after ball spinning, where there is not relative movement between the inner tube and the outer tube as well. As a consequence, to guarantee the interface compatibility of the composite tube during ball spinning, where there is not relative movement between the inner tube and the outer tube before and after ball spinning, velocity boundary condition of the composite tube should meet the following expression.

$$V_1 = V_3, \quad V_2 = V_4 \tag{3}$$

where the corresponding parameters have been interpreted in Fig. 11.

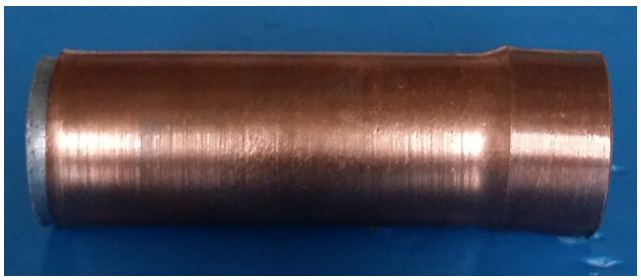

Fig. 10 Al-Cu composite tube subjected to longer ball spinning stroke

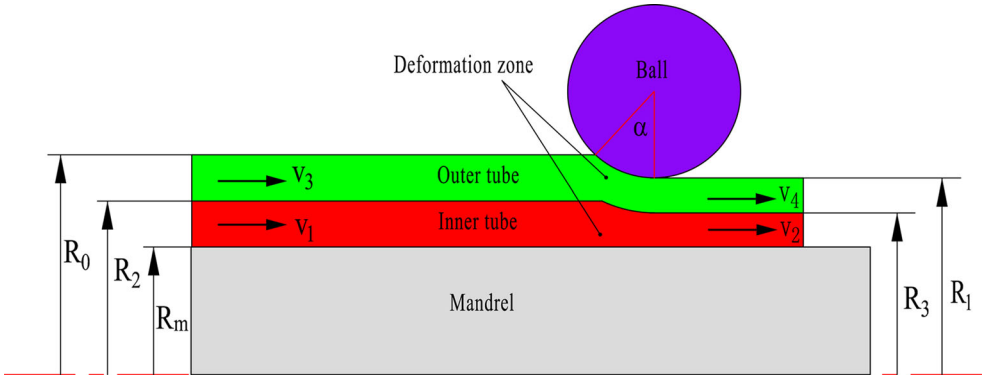

Fig. 11 Velocity boundary condition of the composite tube subjected to ball spinning, where V_1 and V_2 stand for the velocities at the entrance and exit ends of the inner tube, V_3andV_4 for the velocities at the entrance and exit ends of the outer tube, R_0 and R_1 for the outer radius of the outer tube at the entrance and exit ends, R_2 and R_3 for the outer radius of the inner tube at the entrance and exit ends, R_m for the radius of the mandrel

4.3.2 Geometrical condition of composite tubular blank

In the course of ball spinning of the composite tube, the metal material is regarded as incompressibility. In other words, the composite tube must meet the requirement for volume constancy in the plastic deformation. For a given spinning time t, the geometrical condition of the composite tubular blank should satisfy the following expression.

$$\begin{cases} \frac{1}{2}\pi\left(R_0^2-R_m^2\right)V_3t=\frac{1}{2}\pi\left(R_1^2-R_m^2\right)V_4t \\ \frac{1}{2}\pi\left(R_0^2-R_2^2\right)V_3t=\frac{1}{2}\pi\left(R_1^2-R_3^2\right)V_4t \\ \frac{1}{2}\pi\left(R_2^2-R_m^2\right)V_1t=\frac{1}{2}\pi\left(R_3^2-R_m^2\right)V_2t \end{cases} \tag{4}$$

where the corresponding geometrical parameters have been described in Fig. 11.

By combining Eq. (3) with Eq. (4), the following expression can be obtained.

$$\frac{R_0^2-R_m^2}{R_1^2-R_m^2}=\frac{R_0^2-R_2^2}{R_1^2-R_3^2}=\frac{R_2^2-R_m^2}{R_3^2-R_m^2} \tag{5}$$

As a consequence, Eq. (5) stands for the geometrical condition of the composite tubular blank for guaranteeing the interface compatibility during ball spinning.

4.3.3 Steady flow condition of surface metal

It can be noted that Eq. (5) is established on the basis of volume constancy in the plastic deformation of metal material. Therefore, in the case of ball spinning of the composite tube, it is necessary to lead to the steady flow of metal material on the surface of the outer tube in order to guarantee the interface compatibility of the composite tube. As a consequence, the attack angle α should meet the following expression.

$$\alpha=\arccos\frac{d-2(R_0-R_1)}{d}<\alpha_c \tag{6}$$

where d is the diameter of ball, and α_c is the critical attack angle, above which the steady flow of metal material on the surface of the outer tube cannot take place. In other words, if $\alpha>\alpha_c$, Eq. (5) shall not be fulfilled such that the interface compatibility of the composite tube is unable to be satisfied.

4.3.4 Plastic yield condition of composite tube

It can be found from the aforementioned experimental and simulated results that plastic yield of the inner tube and the outer tube plays an important role in the interface compatibility of the composite tube in the course of ball spinning. In other words, the inner tube and the outer tube are simultaneously subjected to plastic yield in order to guarantee the interface compatibility of the composite tube. Accordingly, three principal compressive stresses, which are located in the deformation zone of the inner tube and the outer tube of the composite tube, meet the Mises yield criterion as follows.

$$(\sigma_1-\sigma_2)^2+(\sigma_2-\sigma_3)^2+(\sigma_3-\sigma_1)^2=2\sigma_s^2 \tag{7}$$

Simultaneously, yield strength of the inner and the outer tubes meet the following requirement.

$$\sigma_{so}\geq\sigma_{si} \tag{8}$$

where σ_{so} is the yield strength of the outer tube and σ_{si} is the yield strength of the inner tube.

5 Conclusions

1. Ball spinning of two kinds of composite tubes, including the Al-Cu composite tube and the Cu-Al composite tube, were simulated on the basis of rigid-plastic finite element method. Finite element simulation results indicate that two kinds of composite tubes exhibit a certain similarity in the distribution of the stress and the strain in the deformation zone. However, in the case of interface

compatibility, there exists an obvious difference between the Al-Cu composite tube and the Cu-Al composite tube, where as for the Al-Cu composite tube, the inner aluminum tube, and the outer copper tube keep a good synchronism in terms of plastic deformation.

2. Ball spinning of two kinds of composite tubes, including the Al-Cu composite tube and the Cu-Al composite tube, was implemented on the basis of the process experiment. The experimental results are in good agreement with the simulated ones. In the case of the Cu-Al composite tube, the outer aluminum tube possesses the greater axial elongation compared with the inner copper tube. The phenomenon indicates that the yield strength of the inner and outer tubes plays a significant role in the interface compatibility during ball spinning of the composite tube.
3. According to the experimental and simulated results, the interface compatibility of the composite tube during ball spinning should meet the following requirements, including boundary condition of admissible velocity field, geometrical condition of composite tubular blank, steady flow condition of surface metal, and plastic yield condition of the composite tube.

Acknowledgements The work was financially supported by National Natural Science Foundation of China (No. 51475101).

References

1. Jiang W, Fan Z, Li C (2015) Improved steel/aluminum bonding in bimetallic castings by a compound casting process. J Mater Process Tech 226:25–31
2. Knezevic M, Jahedi M, Korkolis YP, Beyerlein IJ (2014) Material-based design of the extrusion of bimetallic tubes. Comp Mater Sci 95:63–73
3. Wang XS, Li PN, Wang RZ (2005) Study on hydro-forming technology of manufacturing bimetallic CRA-lined pipe. Int J Mach Tool Manu 45:373–378
4. Guo XZ, Tao J, Wang WT, Li HG, Wang C (2013) Effects of the inner mould material on the aluminum-316L stainless steel explosive clad pipe. Mater Des 49:116–122
5. Yu H, Fan Z, Li C (2014) Magnetic pulse cladding of aluminum alloy on mild steel tube. J Mater Process Tech 214:141–150
6. Lapovok R, Ng HP, Tomus D, Estrin Y (2012) Bimetallic copper–aluminium tube by severe plastic deformation. Scripta Mater 66: 1081–1084
7. Xia Q, Xiao G, Long H, Cheng X, Sheng X (2014) A review of process advancement of novel metal spinning. Int J Mach Tool Manu 85:100–121
8. Ma F, Yang H, Zhan M (2010) Plastic deformation behaviors and their application in power spinning process of conical parts with transverse inner rib. J Mater Process Tech 210:180–189
9. Haghshenas M, Jhaver M, Klassen RJ, Wood JT (2011) Plastic strain distribution during splined-mandrel flow forming. Mater Des 32:3629–3636
10. Ma H, Xu W, Jin BC, Shan D, Nutt SR (2015) Damage evaluation in tube spinnability test with ductile fracture criteria. Int J Mech Sci 100:99–111
11. Shan DB, Yang GP, Xu WC (2009) Deformation history and the resultant texture and microstructure in backward tube spinning of Ti-6Al-2Zr-1Mo-1V. J Mater Process Tech 209:5713–5719
12. Mohebbi MS, Akbarzadeh A (2011) Fabrication of copper/aluminum composite tubes by spin-bonding process: experiments and modeling. Int J Adv Manu Tech 54:1043–1055
13. Jiang S, Ren Z, Xue K, Li C (2008) Application of BPANN for prediction of backward ball spinning of thin-walled tubular part with longitudinal inner ribs. J Mater Process Tech 196:190–196
14. Jiang S, Zhang Y, Zhao Y, Tang M, Li C (2013) Finite element simulation of ball spinning of NiTi shape memory alloy tube based on variable temperature field. T Nonferr Metal Soc 23:781–787
15. Zhang GL, Zhang SH, Li B, Zhang HQ (2007) Analysis on folding defects of inner grooved copper tubes during ball spin forming. J Mater Process Tech 184:393–400
16. Kuss M, Buchmayr B (2015) Analytical, numerical and experimental investigations of a ball spinning expansion process. J Mater Process Tech 224:213–221
17. Jiang S, Ren Z, Li C, Xue K (2009) Role of ball size in backward ball spinning of thin-walled tubular part with longitudinal inner ribs. J Mater Process Tech 209:2167–2174
18. Mohebbi MS, Akbarzadeh A (2010) Experimental study and FEM analysis of redundant strains in flow forming of tubes. J Mater Process Tech 210:389–395